Improving irrigation water use and management in large paddy rice fields using SWAT model

Fatuma Muhindo[1], Daniel Otim[1*], Denis Bwire[1, 2], Victo Nabunya[1], Yoronimoh Oketcho[3], Moses Mugisha[3]

(1. Department of Agricultural Mechanisation and Irrigation Engineering, Busitema University, P.O Box 236, Tororo, Uganda;
2. United Graduate School of Agricultural Sciences, Tokyo University of Agriculture and Technology, 3-8-1, Harumicho, Fuchu, Tokyo 183-8538, Japan;
3. Department of Water Resources Engineering, Busitema University, P.O Box 236, Tororo, Uganda)

Abstract: Paddy fields are designed with water impoundments in which their ecohydrological processes are affected by water management practices, the case in the Doho rice scheme, Butaleja District, Uganda, with large paddy fields and farmers facing water management challenges. The water source for this Ugandan scheme originates from Manafwa River, which experiences floods due to climate change, poor drainage, and land use change, affecting paddy production. Flooding deposits silt in the channels. The soil and water assessment tool (SWAT) simulates and simplifies hydrological processes in large paddy fields. The SWAT Model was used in this study to assess irrigation water use and sustainable water management strategies by simulating hydrologic processes within the catchment for a period of 35 years (2015 to 2050) using hydrological data from the Manafwa catchment and assessing future water-use demand. The SWAT output viewer was also applied to analyse water-use scenarios in the catchment. Model calibrations by SWAT-CUP were performed using the data from 2002 to 2008 and then validated with data from 2009 to 2013. The calibration was successfully performed in the SWAT model with Nash-Sutcliffe Efficiency (NSE) of 0.77 and a coefficient of determination (R^2) of 0.79. On the other hand, NSE and R^2 values for validation were 0.55 and 0.7 respectively. Calibration data was used to check model performance, which produced reliable results. Average annual available water in the Manafwa River was 949.5192 m^3 s^{-1} and the crop water requirement of the paddy rice in the Doho rice scheme was 11.053 M m^3. Similarly, the SWAT output viewer showed that the pothole impoundment module improved irrigation water in times of competitive demands and dry seasons. Therefore, implementing desiltation and grassed waterways minimizes soil erosion, a reliable approach for reducing sedimentation in the river and the channels, significantly contributing to water management in such large irrigation schemes.

Keywords: climate change, food security, hydrological processes, land use changes, paddy production, SWAT

Citation: Muhindo, F., D. Otim, D. Bwire, V. Nabunya, Y. Oketcho, and M. Mugisha. 2025. Improving irrigation water use and management in large paddy rice fields using SWAT model. Agricultural Engineering International: CIGR Journal, 27(2): 29-48.

1 Introduction

Globally, rice is one of the most popular cereal crops and staple food for many people (Prodhan and Shu, 2020). Current projections indicate that rice will remain the world's most important staple food in the

Received date: 2024-06-19 **Accepted date:** 2025-02-23

*Corresponding author: Daniel Otim, Department of Agricultural Mechanisation and Irrigation Engineering, Busitema University, P.O Box 236, Tororo, Uganda. Email: danotim@gmail.com.

coming decades (OECD and FAO, 2022). The global rice production by 2023 is projected at a record 520.5 million tons, up more than 2 percent from a year earlier (USDA, 2023). China is the leading rice-producing country with 147 million tons followed by India with 124 million tons (FAOSTAT, 2018), and rice production has extended to other continents, including Africa (USDA, 2023). In sub-Sahara Africa, there is an increase in rice consumption and continuous expansion of irrigated land which calls for the demand for sustainable water management in paddy fields (Tsuchiya et al., 2018). The need for rice production with less water is crucial for food security, and irrigation plays a more significant role in meeting future food needs than it has in the past (Bwire et al., 2025).

In East Africa, Tanzania is the leading rice producer, accounting for 9% (2.6 million tons) of rice production in Africa annually (Materu et al., 2018). This is attributed to the large potential area and water resources for rice production in Tanzania compared with other East African countries. However, many African countries increasingly depend on rice imports due to a rising gap between production and consumption (Materu et al., 2018). Similarly, increasing water withdrawals, spatial and temporal rainfall and runoff variability are contributing to water scarcity in many parts of East Africa (Katic, 2014). Studies indicate that about 20% of all irrigated rice areas will suffer from water scarcity by 2025 (Tuppad et al., 2010).

Additionally, climate change contributes to water scarcity, where water demands increase beyond available water supplies due to its physical limitations in water supplies and insufficient water management structures (Hoekstra et al., 2012). The situation is worse for a country like Uganda, whose agriculture is heavily rain-fed (Bwire et al., 2017; Bwire et al., 2022b). According to Mwaura and Muwanika (2018), only 1% of farmers in Uganda are involved in irrigation of which 55% are in the Eastern region. Much as climatic conditions for the production of both irrigated and upland rice are conducive in Uganda with mean annual rainfall of 1,180 mm and 15% of her surface area covered by fresh water resources (Hong et al., 2021), rainfall and water supply are majorly in abundance at Doho rice scheme in the first cropping season with farmers frequently suffering from flooding while scarcity of water is experienced in the second season (Angella et al., 2014). Therefore, it necessitates farmers to intervene in water management through drainage during flooding instances in crop fields (Mwaura and Muwanika, 2018). Farmers' plots in Doho Rice Irrigation Scheme receive up to 50mm daily ponding of irrigation water thrice a week over four months translating to 2,400mm of water applied which is way above the average rice water requirements of 700mm per season (Onen et al., 2022). The eastern region of Uganda is the leading national rice producer in Uganda with annual production approximately 3.6 metric tons ha^{-1} (Kajonphol et al., 2018). However, rice yields in Uganda are remarkably low compared with other countries such as Rwanda and Sudan (Kajonphol et al., 2018). Likewise, the Doho rice scheme in Butaleja district, Uganda, has experienced reduced yields in recent years due to land use changes and floods in the Manafwa River catchment affecting rice production (MWE, 2012). The subsequent study by Erima et al. (2022) shows that changes in land-use/cover have translated to increased annual surface runoff, sediment yield, and water yield making commercial farmlands highly vulnerable and subsistence farmlands moderately to highly vulnerable. Similarly, local farmers have inadequate knowledge to improve crop productivity through irrigation water use and management strategies (Liyantono et al., 2013).

Therefore, farmers need to be supported through knowledge transfer and decision support tools to improve irrigation water use, management, and conservation approaches, including Alternate wetting and drying irrigation (AWD), to sustain increases in paddy rice yields with a concurrent reduction of water footprint to ensure food security (Bwire et al., 2022b; Bwire et al., 2022a; Bwire et al., 2025). Several tools

have been developed to assess water management and use in large paddy fields. These models include MIKE System Hydrology European (MIKE SHE), Hydrological Simulation Program-FORTRAN (HSPF), and WEAP Model. The challenge with some of these models is that they are not designed to simulate wetting conditions with water flooding commonly practiced in paddy fields (Tsuchiya et al., 2018). The SWAT is a hydrological model used in assessing the land and water resources sustainability, in consideration of agricultural production in watershed scale (Dechmi et al., 2012). Eco hydrological simulations and related water assessments have been used globally in addressing several water-resource challenges (Akoko et al., 2021). Additionally, several researchers have studied and improved hydrological processes of large paddy fields using SWAT model, especially in Eastern Asia (Sakaguchi et al., 2014). The model has several applications in agricultural watersheds, water resources and related environmental assessments. The model has been applied to evaluate land use changes, erosion, climate change, and water quality (Van Griensven et al., 2012). Further, it has been involved in other research areas, such as modifications of curve number and wetland applications, with best management practices highlighted in several peer-reviewed journals (CARD, 2019). While the model applications have proved effective and reliable in other continents, its application results in Africa have high uncertainty (Gassman et al., 2014). Nevertheless, the model is suitable for modelling hydrological processes in large-scale and data-scarce areas (Gassman et al., 2007).

According to McCuen et al. (2006), measured data is not replicated by hydrologic models to perfection and calibration is undertaken to reduce discrepancies to a minimum. Model verification is the determination of the correctness of simulated output through comparison with observed data, therefore, verification of a model is a measure of the model's performance (Schulze, 2011). For acceptable simulations, the minimum coefficient of determination (R^2) should be 0.60 and the Nash–Sutcliffe coefficient of efficiency (NSE) should be close to unity (Otim et al., 2020). However, model goodness-of-fit is better evaluated by the NSE (Nash and Sutcliffe, 1970) than the R^2 because R^2 is insensitive to additive and proportional differences between model simulations and observations (Harmel et al., 2014). According to Moriasi et al. (2007), model performance index is evaluated for NSE values based on general performance ratings of very good ($0.75<NSE\leq1.00$), good ($0.65<NSE\leq0.75$), satisfactory ($0.50<NSE\leq0.65$), and unsatisfactory ($NSE\leq0.50$). Furthermore, model performance is examined based on its ability to maintain similarities in shapes and distributions of peaks between observed and simulated values (Kim et al., 2014).

This study focused on the application of the SWAT Model to evaluate water management strategies and improve irrigation water use in large rice paddies of the Doho rice scheme. Specifically, the research aims to: 1) assess water availability for irrigation in the scheme, and 2) evaluate sustainable irrigation water management scenarios i.e. implementing the pothole impoundment module, desiltation and grassed waterways using the SWAT Model. The model has been applied globally to assess water quality and associated challenges due to the availability and support of several software tools in preparation of input data, checking of errors in a simulation, and calibration of parameters for SWAT model simulation. As a result, the users can easily apply the model (Sakaguchi et al., 2014). The results from this study are significant and a potential guide to administrators, engineers, and water associations in developing sustainable management watershed for large paddy fields (Tsuchiya et al., 2018).

2 Materials and methods

A description of the materials and methods employed in this study is presented in this section while the workflow scheme of this study is shown in Figure 1.

2.1 Geographical location of study area

The Doho rice scheme lies between altitudes of 1,100 to 1,220 m above sea level (Longitude 34°02' E; Latitude 0°88' N) within Lake Kyoga basin covering an area of 494.2 km^2 with about 4,340 farmers growing rice in the scheme as shown in Figure 2. It is the largest irrigation scheme in Uganda designed to distribute irrigation water to 1,000 ha of paddy fields. The scheme comprises of 11 blocks connected by three channel types: main, sub, and tertiary. The main channel provides irrigation water from the Manafwa River to the scheme (Bwambale et al., 2019). Then, it transmits water to sub-channel branches providing irrigation water to each block. Each of the blocks contains one sub-channel consisting of 5 to 15 smaller zones called strips surrounded by a tertiary channel providing water for 20-30 farmers and unto the drainage channel for excess water from the blocks serving the tails end blocks (Bwambale et al., 2019). The drainage channel acts as a tertiary irrigation channel for the adjacent strip. After flowing through paddy fields, water is collected into the main drainage through the tertiary and sub-drainages into the Manafwa River (Namyenya et al., 2014).

2.2 Data sources

Daily observed rainfall and River Manafwa discharge data for the period 1996-2019 were obtained from Uganda National Meteorological Authority (UNMA) and Ministry of Water and Environment, Directorate of Water Resources Management respectively. On the other hand, the Digital Elevation Model for the study area was obtained from the Department of Surveys in the Ministry of Lands, housing and Urbanization whereas soil data was downloaded from the Food and Agricultural Organisation (FAO) database with land use maps to a scale of 1:5,000 and Landsat+ETM 2019 data obtained from Google maps and Google Earth respectively. The soil texture within the study area includes sandy clay loam, clay, clay loam, sandy loam, and sand whereas the land slopes range from 1.3% to 39.9%. On the other hand, land use/ cover within the study area includes water, urban, forests, and agriculture.

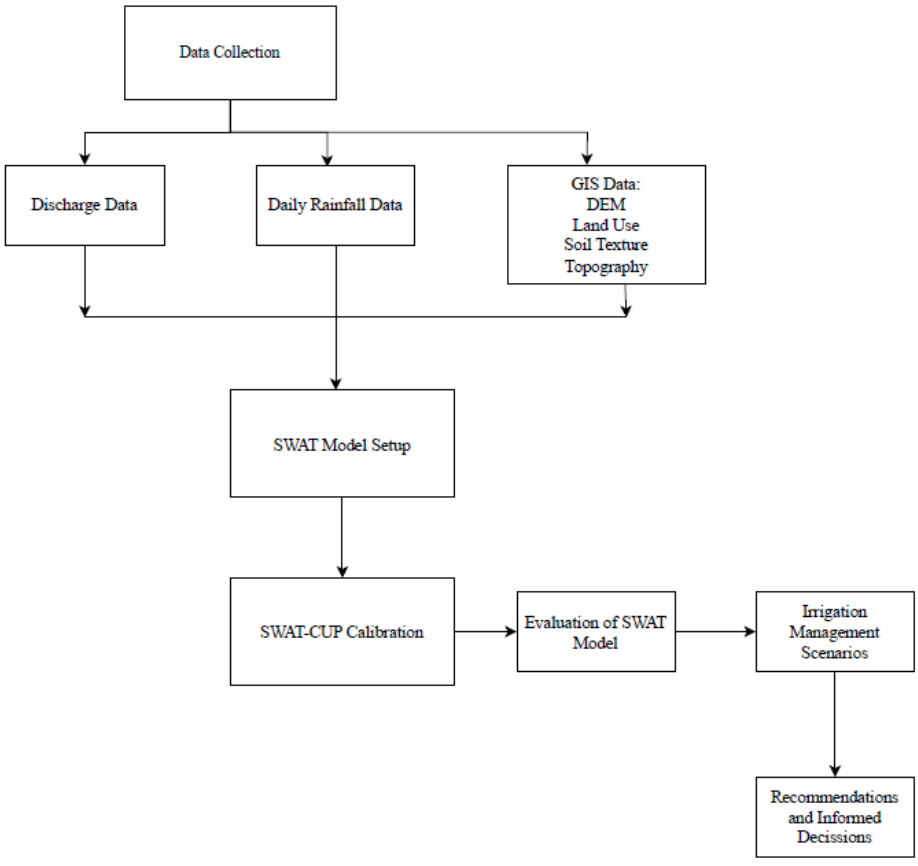

Figure 1 Workflow scheme of study

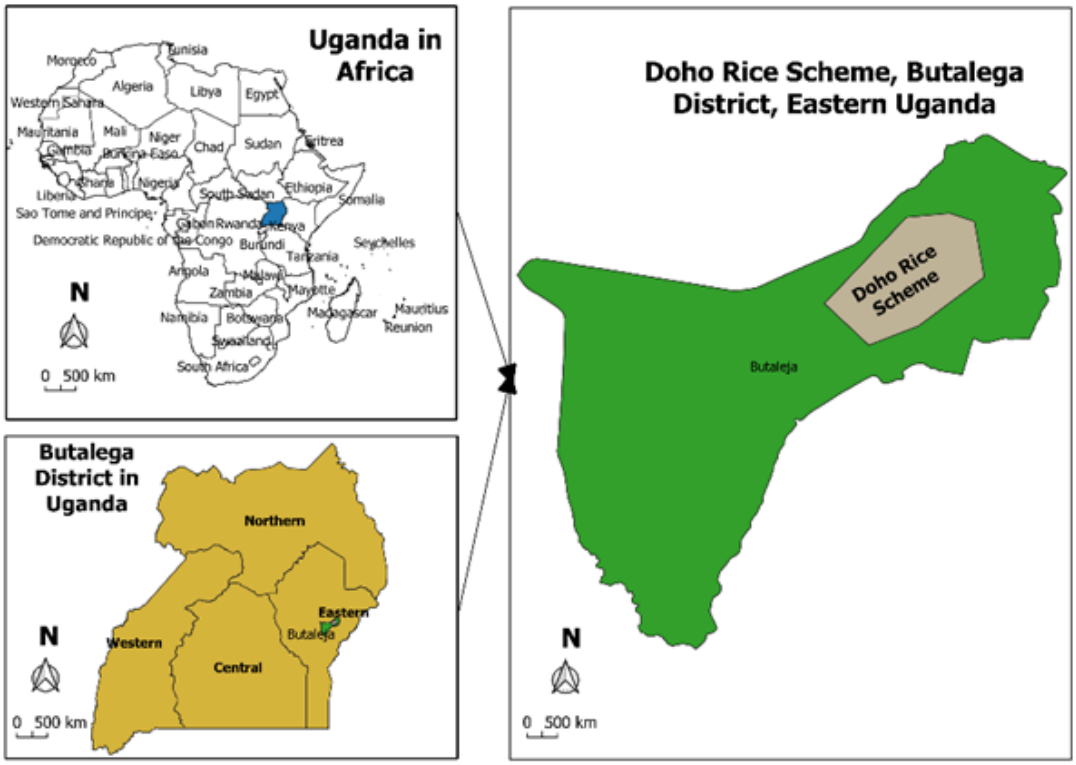

Figure 2 Geographical location of study area in Uganda, Map developed from QGIS 3.28.1

2.3 The soil water assessment tool (SWAT) model

The SWAT model is a semi-distributed, eco-hydrological model that simulates water flow, nutrient fluxes, pesticides, carbon dynamics, and plant growth using the daily time step of the watershed scale (Ouyang et al., 2020; Wei and Zimmermann, 2017). The hydrological cycle within the watershed is simulated in two phases: (1) land phase and (2) routing phase. The basin is divided into sub-basins for modelling the land phase, which is further subdivided into one or more hydrologic response units (HRUs) (Tuppad et al., 2010). HRUs represent relatively homogeneous land use land cover (LULC) areas and soil types. The inherent characteristics of HRUs define the hydrological response of sub-basins. For each time step, the contributions to the discharge at sub-basin outlets are controlled by the water balance of the HRU (land phase). The river network connects various sub-basin outlets while the routing phase assesses water movement through the network (Neitsch, 2005). SWAT uses the Soil Conservation Services (SCS) method that assesses the relations between land use and soil characteristics; thus it is suitable for assessing impacts of land use change (Neitsch, 2005).

2.4 The SWAT model in-put data sets

Input data for the SWAT model consist of a digital elevation model (DEM), land cover/use map, slope map, and soil map prepared using ArcMap 10.6 (Figure 3). The maps were projected to Universal Transverse Mercator (UTM). Arc SWAT 2012 was used through an ArcMap 10.6 user interface. The process of model set up was divided into four phases: watershed delineation, hydrologic response unit (HRU) definition, weather data definition, and writing input tables.

The DEM was used for delineating the watershed, creating the sub-basins, stream network, and topographic characteristics, such as elevation, slopes, and slope lengths. The DEM was obtained from the Department of Survey in the Ministry of Lands, Housing, and Urbanization in Uganda, with a spatial resolution of approximately 30 m, as the source of topographic information to run SWAT. The land use, soil, and slope maps raster data sets were input to the SWAT model and subsequently run. The grid field on which reclassification was based was set to VALUE. The land use dataset was reclassified into SWAT land

use themes. The land use in the catchment was: agriculture (56.36%), forest (42.46%), settlement (0.60%) and water (0.58%) as indicated in Table 1.

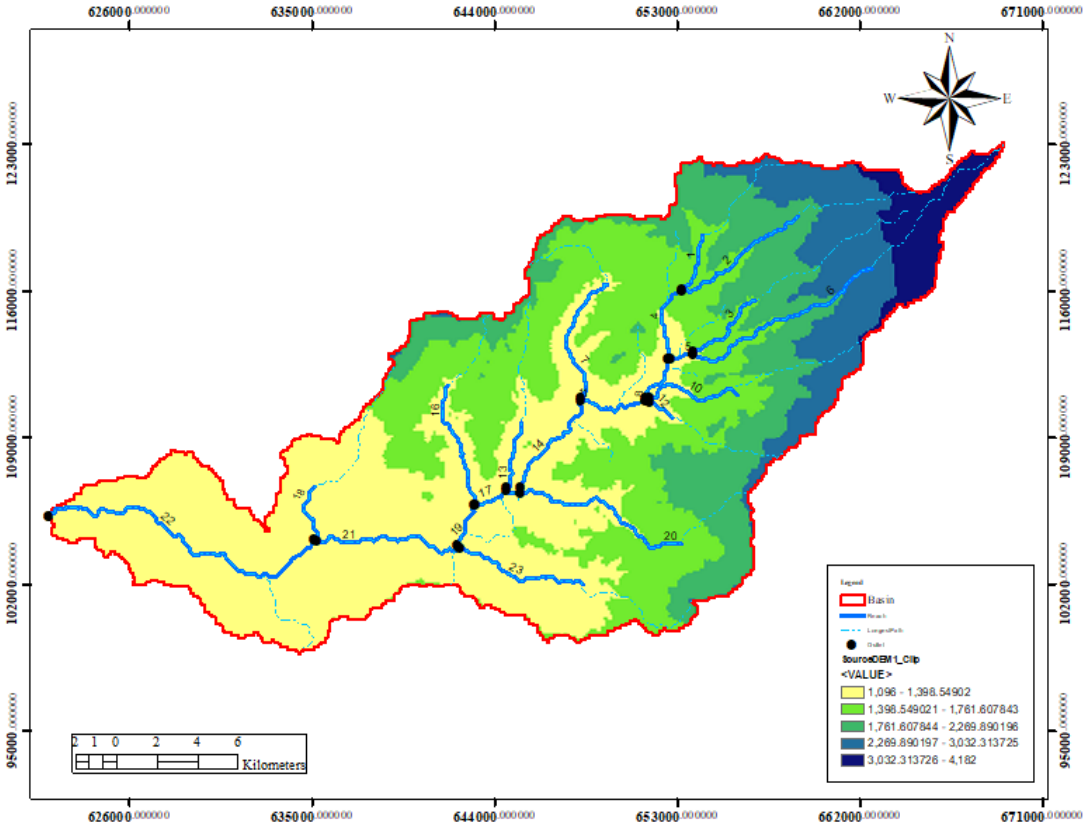

(a) DEM

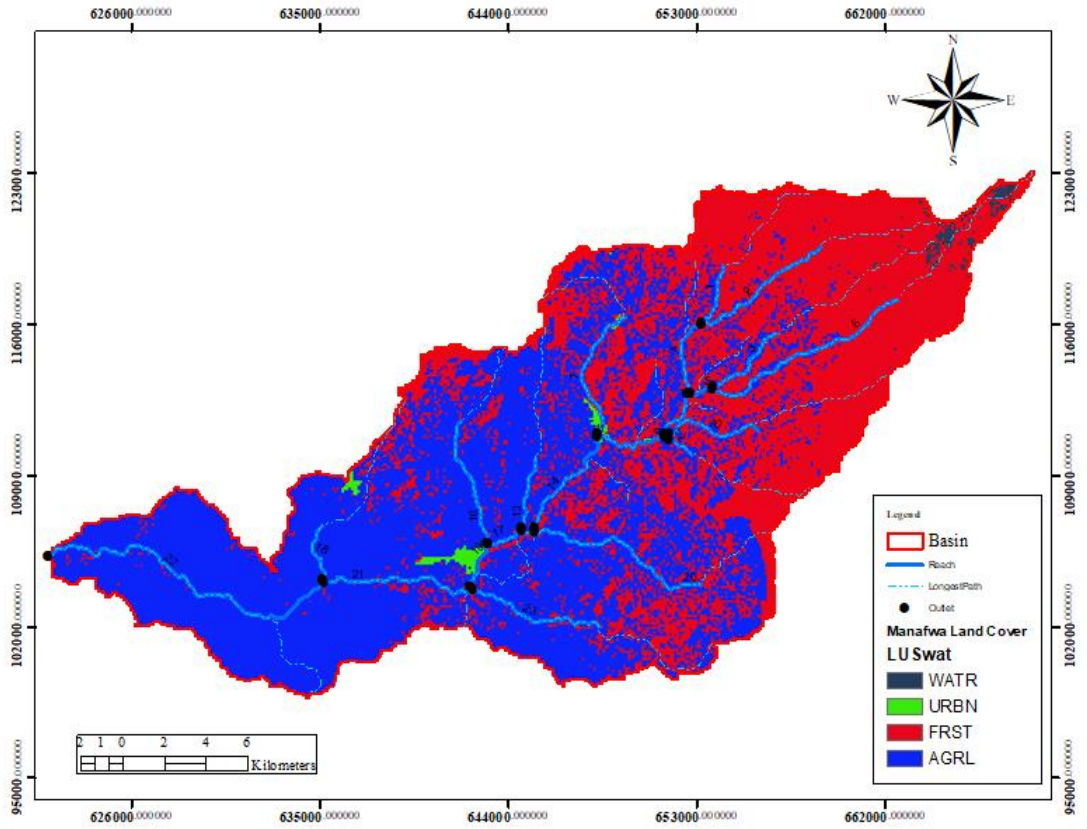

(b) Land cover

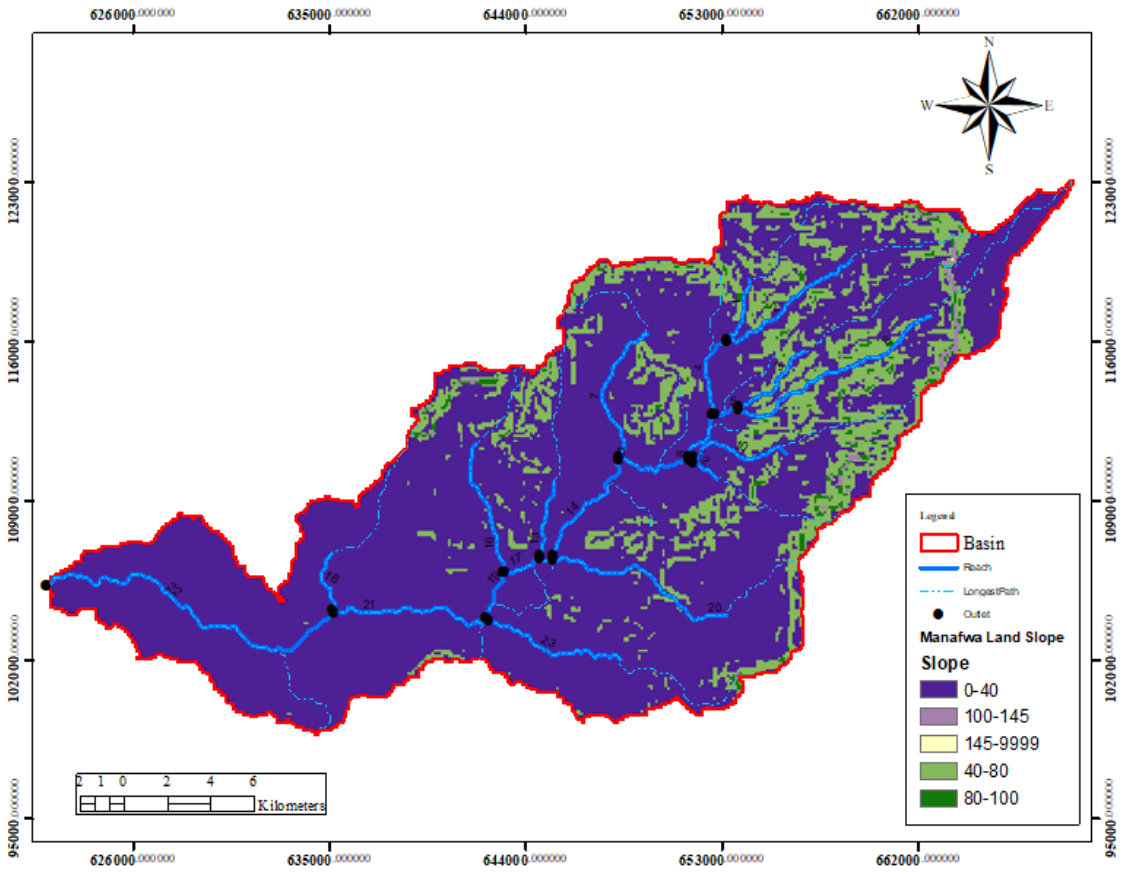

(c) Slope

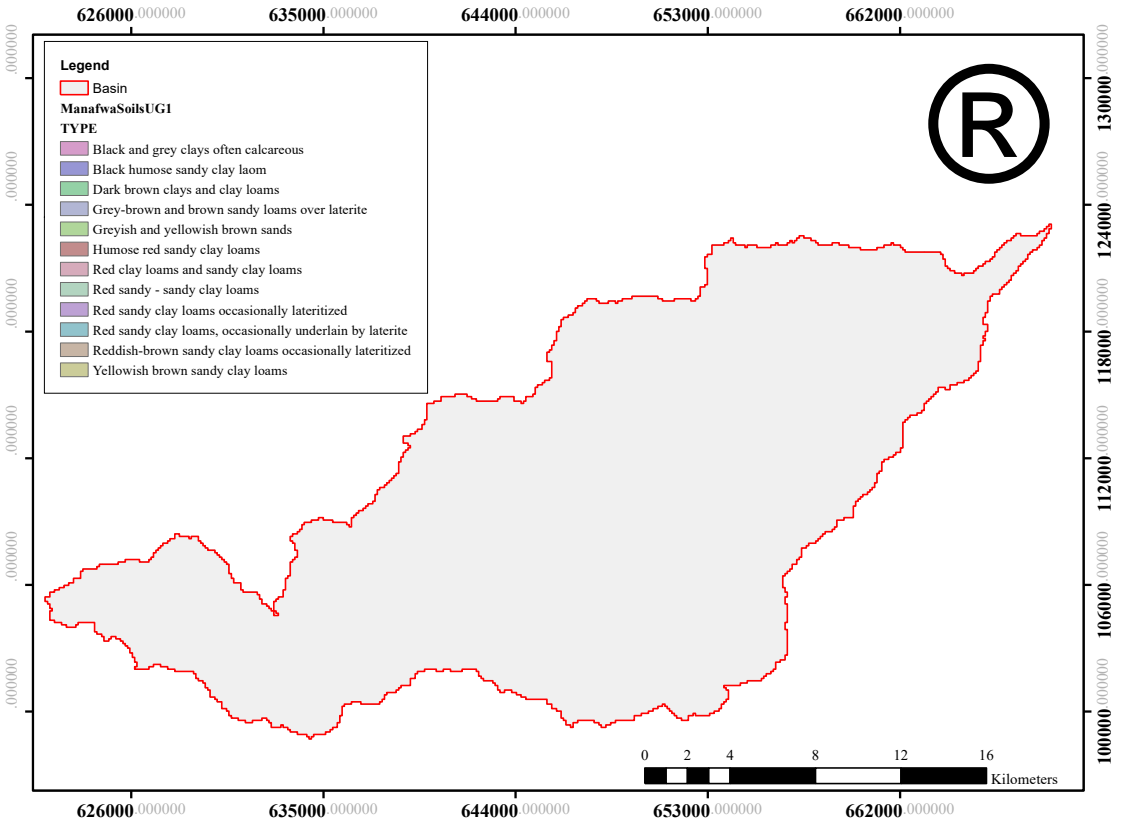

(d) Soil map

Figure 3 Manafwa River catchment

Table 1 Spatial distribution of the land use categories of the Manafwa river catchment

S/N	Land use	SWAT code	Percentage (%)
1	Water	WATR	0.58
2	Settlement	URBN	0.60
3	Forest	FRST	42.46
4	Agriculture	AGRL	56.36

The model was used to categorize soils in different ways, for example, peat sandy and clay, red sandy clay loam soils, among others (Figure 3d). Red sandy clay loam soil is found up stream of the catchment, whereas black and grey clays often calcareous is found downstream of the catchment and multiple slope options were chosen during slope discretization. Three slope gradient classes were used: 0 – 2%, 2% – 60% and 60% – 99%. The land use, soils, and slope definition process were completed by the overlay of the land use, soils and slope datasets and creation of HRU feature class. HRU definition is necessary for segmenting the watershed into smaller, homogeneous units and the approach provides an efficient method of pre-computing a hydrologic response for later use (The Nature Conservancy, 2023).

Similarly, the HRUs were created by using land use, slope gradient, and soil (Figure 3b, Figure 3c, and Figure 3d). Several choices were available to create these HRUs using SWAT: these focused either on dominant HRUs or on the minimum limits for each input variable. The HRUs were defined using thresholds, 5% land use, 0% soil to account for small urban area in the catchment and 5% slopes and 349 HRUs were generated. However, we attempted to show the effect of soil, land cover, and slope gradient on hydrological simulations, and 0% was chosen as a minimum percentage of soil class over the watershed area to integrate the maximum information related to the soil, and 5% as the minimum percentage of land use and slope. The number of elevation bands with minimum ranges were set to default. The process was completed by creating HRUs and writing HRU reports.

2.5 Model sensitivity analysis, calibration and validation

The SWAT model was manually calibrated for the long term annually. The hydrological cycle of the catchment was simulated from January 1998 to 31st Dec 2013. Runoff calibrations were performed using the SWAT-CUP parameter solution program (Parasol) (Abbaspour et al., 2015) based on an auto calibration method that stochastically accounts for most sources of uncertainty and expresses the uncertainty in parameters in uniform distributions. The uncertainties in model output variables were expressed as 95% probability distributions (95PPU) using Latin hypercube sampling (Tang et al., 2021). Calibration results were evaluated based on the p-factor (ranges between 0 and 100) and an R-factor (varies between 0 and infinity). In the first iteration, four parameters were selected for optimization. The parameters included groundwater lag time, initial SCS curve number for moisture condition, baseflow alpha factor, threshold depth of water in the shallow aquifer required to initiate return flow, soil bulk density, available soil water, and soil hydraulic conductivity. The number of simulations was set to 10. The sub-basin was set to the catchment level, with the objective functions including the NSE, p-factor, r-factor, coefficient of determination, and coefficient of determination multiplied by the regression coefficient. Computation of the NSE was based on the method proposed by Nash and Sutcliffe (1970) while computation of the coefficient of determination was based on the method presented by Nagelkerke (1991).

The simulation comprised three periods: three years (January 1998 to December 1999) for model initialization (warm-up), two years for calibration, and two years of validation. Sensitivity analysis was used to identify key parameters affecting model performance and was important in model parameterization (Song et al., 2015). Thus, reducing

the number of parameters to be included in calibration is possible, which minimizes the calibration efforts and increases the probability of converging towards a more powerful combination (Arnold et al., 2012; Bouslihim et al., 2019).

The p-value and t-statistic were used to evaluate the significance of the relative sensitivity. A larger absolute t-statistic means a higher sensitivity, and a p-value close to zero represents higher significance (Abbaspour et al., 2015). The coefficient of determination (R^2) and Nash–Sutcliffe Efficiency (NSE) were used to evaluate the accuracy of calibration and validation. The R^2 values vary from zero to one with a value of one representing a perfect correlation, while zero indicates no correlation. NSE values range between negative infinity and one (Bouslihim et al., 2019; Moriasi et al., 2007) with values closer to one being better estimates of modelled streamflow (Geza and McCray, 2008). The NSE function was used as the optimization function during calibration with a minimum threshold for the behavioural solution at 0.50.

Likewise, validation involves checking if the calibrated model could reproduce sufficient simulations. Statistical functions used in calibration to determine model efficiency were also used for validation, which was performed by time series datasets not used in calibration. Studies note that both datasets used for calibration and validation should include wet and dry years, but this is difficult to achieve (Arnold et al., 2012). However, Santhi et al. (2005) recommends 19 as the wet period used for calibration to achieve high runoff events. While no guiding principles exist for separating data for calibration and validation, the minimum period required for calibration and validation should be considered. The validation was performed from 2009 to 2013 using the same parameters obtained from calibration step of this study.

Table 2 List of calibration and sensitivity parameters

Parameters	Type	Original	Range(min)	Range(max)	Best	Parameter Description
CN2.mgt	R	36-86	1.04	1.07	38.12-91.05	Curve number
SOLAWC.sol	R	0.09-0.25	1.35	1.43	0.13-0.35	Available water capacity
RCHRG_DP.gw	v	0.02	0.10	0.12	0.11	Deep aquifer percolation factor for ground water recharge
ALPHA_BF_DP.gw	v	0.9	0.12	0.19	0.15	Base flow-deep percolation alpha factor for groundwater recharge
CNCOEF.bsn	v	0.5	0.52	0.55	0.52	Curve Number runoff coefficient in the basin
ALPHA_BF.gw	v	0.005	0.00	0.02	0.0008	Base flow-deep alpha factor for groundwater recharge
GW_DELAY.gw	v	5	36.83	39.39	38.22	Groundwater
ESCO.hru	v	0.95	0.98	1.00	1.00	Soil evaporation compensation factor in the HRU
EPCO.hru	v	1.00	0.71	0.76	0.73	Plant uptake compensation factor in the HRU
SURLAG.bsn	v	4	14.77	16.75	16.67	Surface runoff lag coefficient

Where: HRU- Hydrologic Response Units.

Similarly, there were mainly three sources of uncertainties associated with hydrologic modelling: uncertainties in the observed data, data used in calibration, and data used in the conceptual model and model parameters. In sequential Uncertainty Fitting (SUFI-2), the uncertainties are quantified by the p-factor, the percentage of data bracketed by the 95% prediction uncertainty (95 PPU). The 95 PPU is calculated at 2.5% and 97.5% levels of the cumulative distribution of an output variable, disallowing 5% of the very bad simulations (Arnold et al., 2012). The r-factor can also be used to quantify uncertainty (i.e., the 'width' of 95% probability band). SUFI-2 brackets the measured data with the smallest r-factor variable (Abbaspour et al., 2015). When the r-factor and p-factor are within the required limits,

other statistical analyses can be used to check the consistency between measured and observed values.

Finally, SWAT calculates the water balance for each HRU, sub-basins, and the entire catchment generated for the calibration period. The water balance components include rainfall, evapotranspiration, surface runoff, lateral flow into the stream, groundwater contribution, water yield, soil water, percolation below the root zone and total water losses.

2.6 Estimation of water availability for irrigation in the scheme

The curve number plays a significant role in determining available water in the stream and how much is lost. The curve number for the catchment was generated from the soil, Land Use Land Cover (LULC), and DEM maps (Figure 3a, Figure 3b, Figure 3c). SWAT mainly uses the water balance equation to simulate runoff, sediment, chemical, and pesticides transported within a watershed (Donmez et al., 2020). The SWAT model partitions the watershed into two parts, (1) the land phase hydrologic cycle and (2) the routing phase. In the land phase, the model governs the amount of surface runoff generated and eroded sediment going into the main channel of each subbasin (Supakosol and Boonrawd, 2020). In the routing phase, the model simulates the water and sediment movement through the network to the watershed outlet (Figure 4).

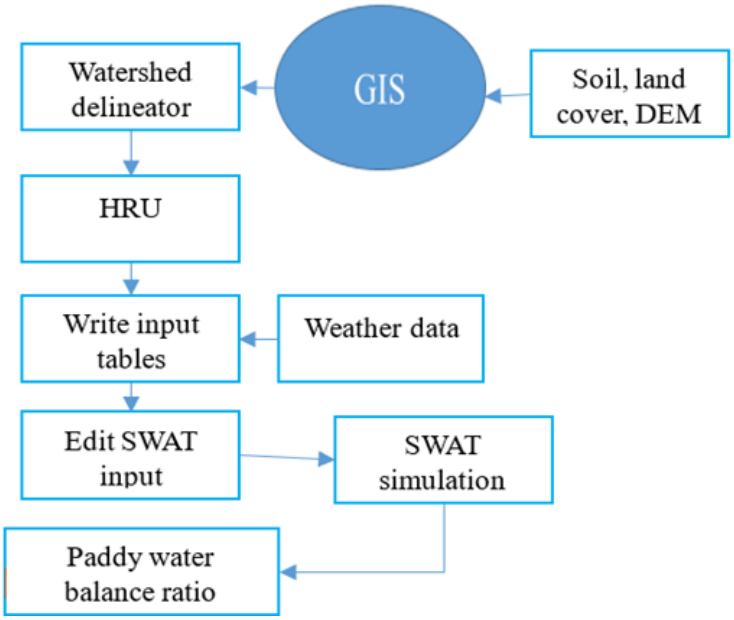

Figure 4 Illustration of steps for estimation of paddy water availability and water balance ratio

2.7 Determination of crop water requirement for paddy rice in the scheme

Paddy rice requires more water than other crops (Bwire et al., 2022a). Crop water need is the depth of water required to meet the water consumed through evapotranspiration by crop growing in large fields under non-restricting soil conditions includng soil and fertilizer. The reference crop water requirements, ET_o, was obtained after running the SWAT ERROR CHECK. This study considered season one (October - March) due to high irrigation water use in those months since the precipitation is relatively low to support paddy rice farming. The crop water requirement for season one (October - March) was determined using FAO Penman-Monteith and crop factors obtained from FAO (1989) for each crop development stage.

$$\mathbf{ET_o}=\frac{\mathbf{0.408}[(\boldsymbol{R_n}-\boldsymbol{G})+\boldsymbol{\gamma}\left(\frac{\mathbf{900}}{\boldsymbol{T}+\mathbf{273}}\right)*\boldsymbol{u_2}(\boldsymbol{e_s}-\boldsymbol{e_a})]}{[\boldsymbol{\Delta}+\boldsymbol{\gamma}(\mathbf{1}+\mathbf{0.34}\boldsymbol{u_2})]} \quad (1)$$

Where: ET_o is the reference crop evapotranspiration (mm day^{-1}), R_n is the net radiation at the crop surface (MJ m^{-2} day^{-1}), G is the soil heat flux density (MJ m^{-2} day^{-1}), T is the air temperature at 2 m height (°C), U_2 is the wind speed at 2 m height (m s^{-1}); e_s is the saturation vapor pressure (kPa), e_a is the actual vapor pressure (kPa), Δ is the slope of

vapor pressure curve (kPa °C^{-1}), and γ = psychometric constant (kPa °C^{-1}),

Then,

$$ET_c = K_c ET_o \quad (2)$$

Where ET_c *is the* crop water requirement for paddy rice (mm day^{-1}), K_c is the crop coefficient, and ET_O, reference evapotranspiration (mm day^{-1}).

2.8 Optimization of water management scenarios

The model uses the pothole impoundment module to simulate water management scenarios. Hydrological processes of paddy fields differ from other land uses due to rainfall and irrigation water stored in the ground as an impoundment during growth seasons (Chen et al., 2013). A pothole refers to a deep and round hole or a pit–a depression that can receive surface runoff from the related HRUs (Xie and Cui, 2011). However, the potholes in this scenario were assumed as cone-shaped pits that temporarily store rainfall (Ouyang et al., 2020). The five water sources contributing to the ponding conditions were rivers, reservoirs, shallow aquifers, deep aquifers, and outside water sources. Considering the hydrological cycles and diffuse pollution relationship (Ouyang et al., 2020), the pothole module assessed was based on the modified module indicated on the original SWAT model as follows:

$$V_i = V_{i-1} + V_{flowin} + V_{pcp} - V_{flowout} - V_{eva} - V_{inf} \quad (3)$$

where; V_i is the water stored in the pothole on the day i (m^3), V_{i-1} is the water stored in the pothole on day i-1 (m^3), V_{pcp} is the volume of precipitation (m^3), V_{flowin} is the volume of irrigation flow (m^3), $V_{flowout}$ is the volume of overflow or drainage flow (m^3), V_{eva} is the water loss via evaporation (m^3), and V_{inf} is the water infiltrated into the soil (m^3).

The size of the pothole based on conditions above was estimated using the formula:

$$SA = \left(\frac{\pi}{10^4}\right)\left(\frac{3V}{\pi.slp}\right)^{\frac{2}{3}} \quad (4)$$

The surface area of each pothole with the available water in the sub-basin was estimated through:

$$\mathrm{SA} - \text{Area hru} \quad (5)$$

where, V is the volume of water stored in the sub-basin (m^3), SA is the surface area of water in the pothole (ha), and Slp is the slope of the HRU (m m^{-1}).

The surface area of water was assumed to be equal to the area of the HRU (ha).

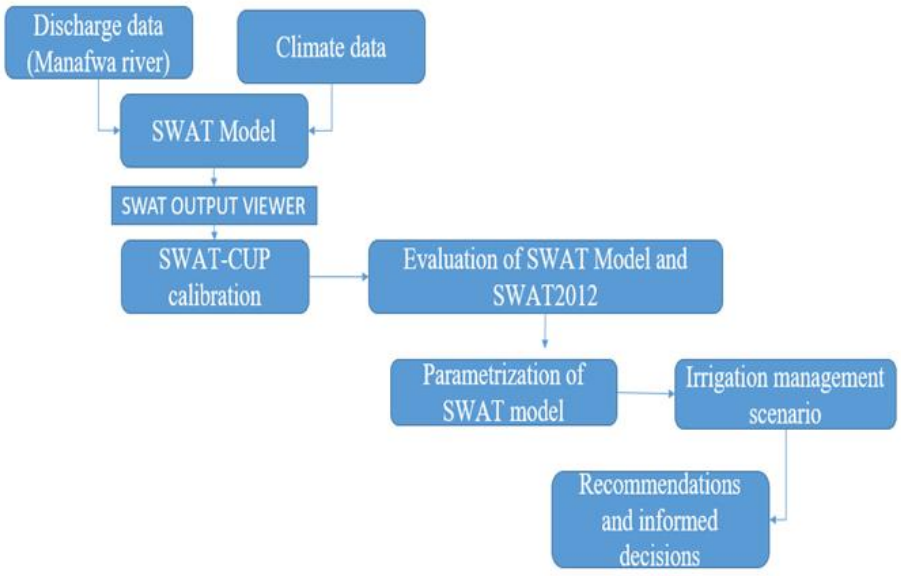

Figure 5 Illustration for the optimization of irrigation water management scenarios

3 Results and discussion

3.1 Model calibration and validation

The long-term calibration (2002-2008) and validation (2009–2013) results for measured and simulated annual flow data for the catchment are shown Figure 6a and Figure 6b respectively.

The model performance in the calibration phase

shown in Figure 6a was very good with the NSE and R^2 values of 0.77 and 0.79 respectively, with the P-factor and r-factor of 45% and 58% from the rainfall stations. In addition, the similarity in shape and distribution of peaks between observed and simulated values was adequately maintained.

Similarly, the NSE and R^2 values for validation (Figure 6b) were 0.55 and 0.70, respectively, with p-factor and r-factors of 40%, and 56%, respectively and the similarity in shape and distribution of peaks between observed and simulated values was adequately maintained. Therefore, model performance was satisfactory. However, the NSE of the calibration was better compared with values in the validation. This observation is consistent with the study conducted by McCuen et al. (2006) who noted that measured data is not replicated by hydrologic models to perfection and calibration is undertaken to reduce discrepancies to a minimum. Hence, the reason as to why the NSE of the calibration was better compared with values in the validation. The optimum value of the most sensitive parameter CN2 was small, which indicates that the soils had high infiltration rate, and stream flow is generated when the soils are saturated.

In both cases, the NSE and R^2 values exceeded the recommended threshold of 0.50 (Moriasi et al., 2007) and 0.60 (Otim et al., 2020). Thus, the validation and calibration results showed that the model assessed well the stream flow at the basin scale in the catchment area. The paddy module in SWAT was activated to represent the water balance for large paddy fields (Tsuchiya et al., 2018). The model was accurately simulated to check paddy module performance and was within the reasonable range of 0.5-1.0.

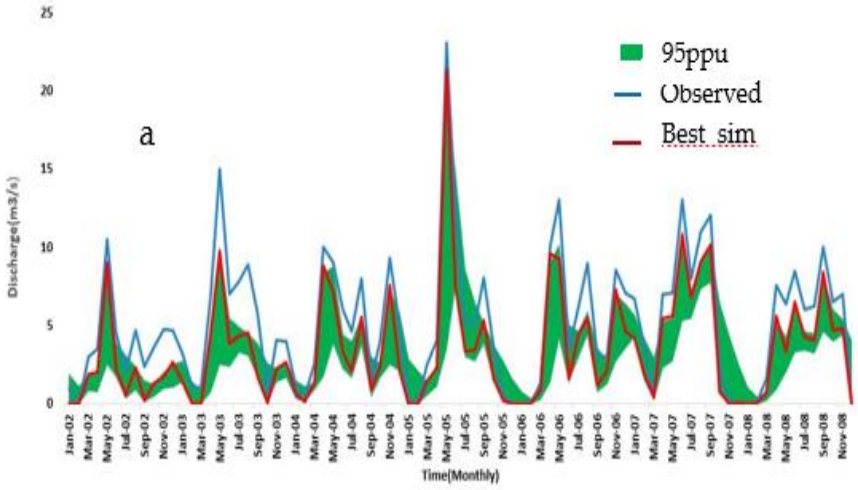

(a) Calibration

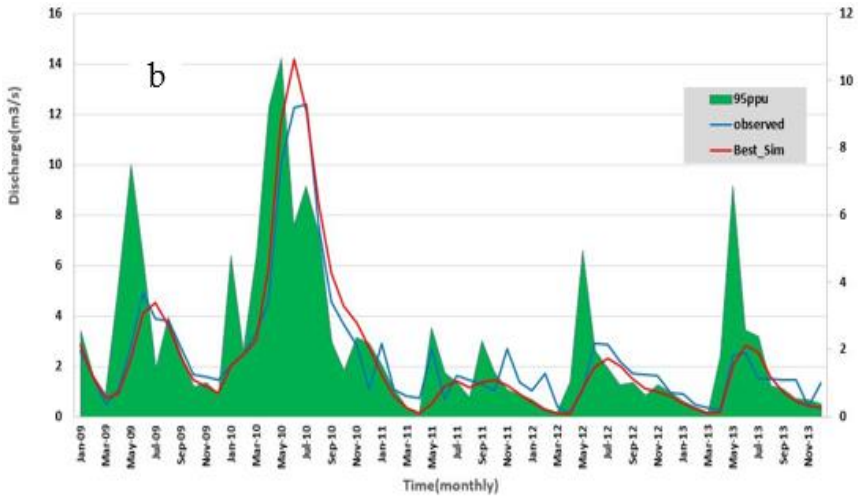

(b) Validation

Figure 6 Calibration and Validation of River Manafwa catchment

3.2 Water availability for irrigation in the scheme

The water balance of Manafwa catchment was extracted from the SWAT output file (output. Subfile). The results of simulated average monthly rainfall from 1998 to 2013 are shown Figure 7b.

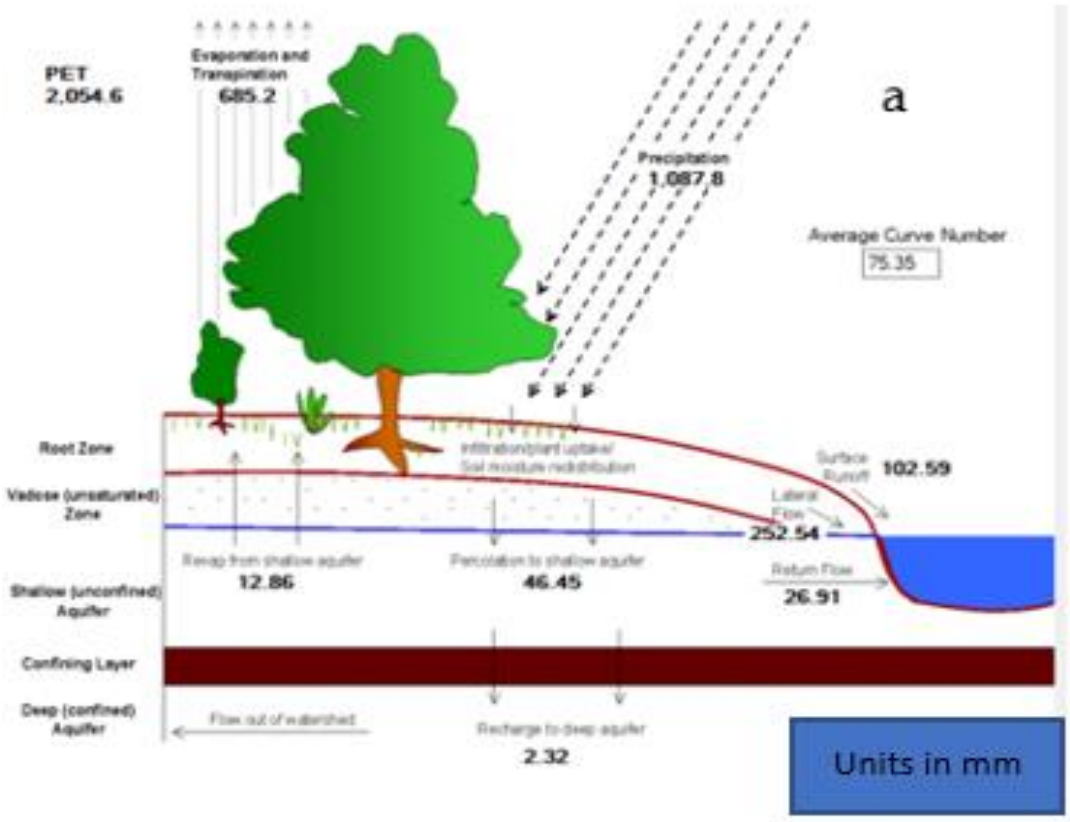

(a) The hydrological water balance cycle

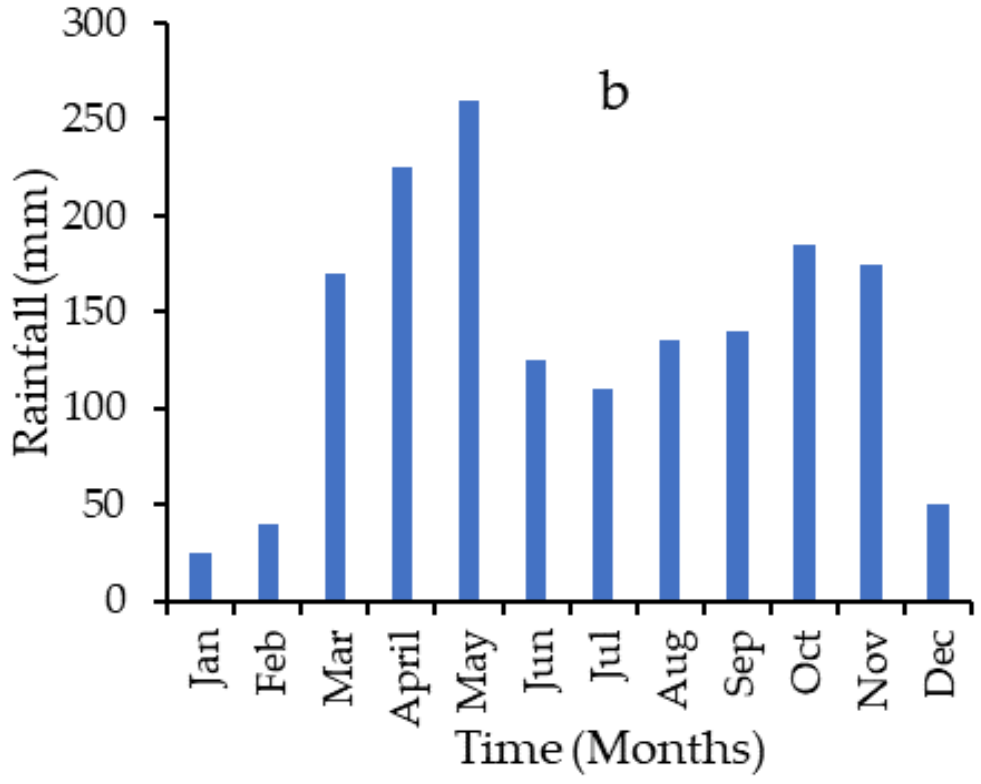

(b) The average monthly rainfall of the Manafwa River catchment

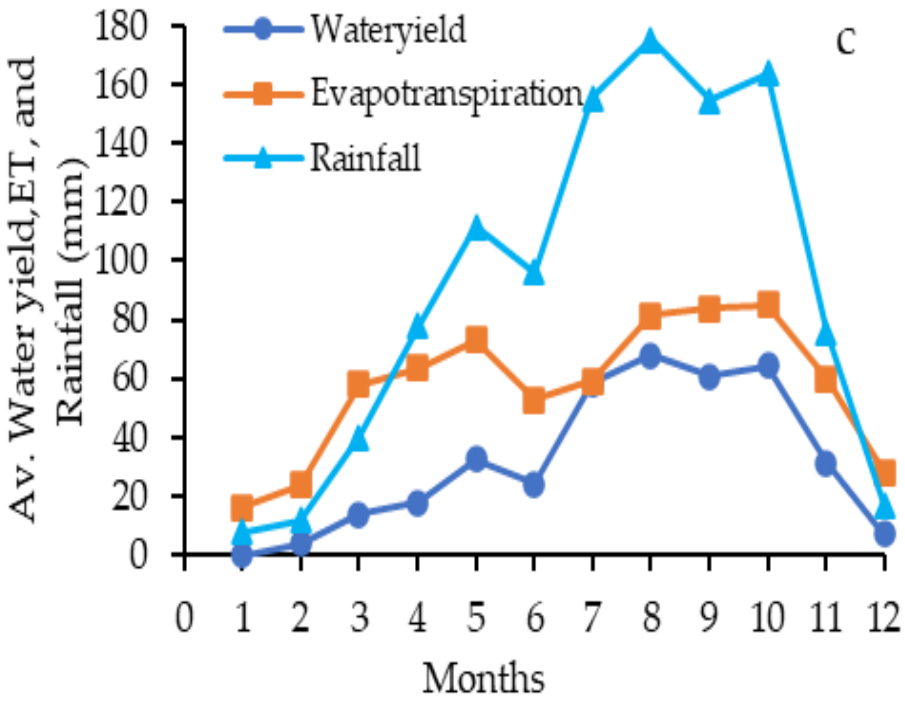

(c) Simulated average water yield and crop water requirements from 1998 to 2013

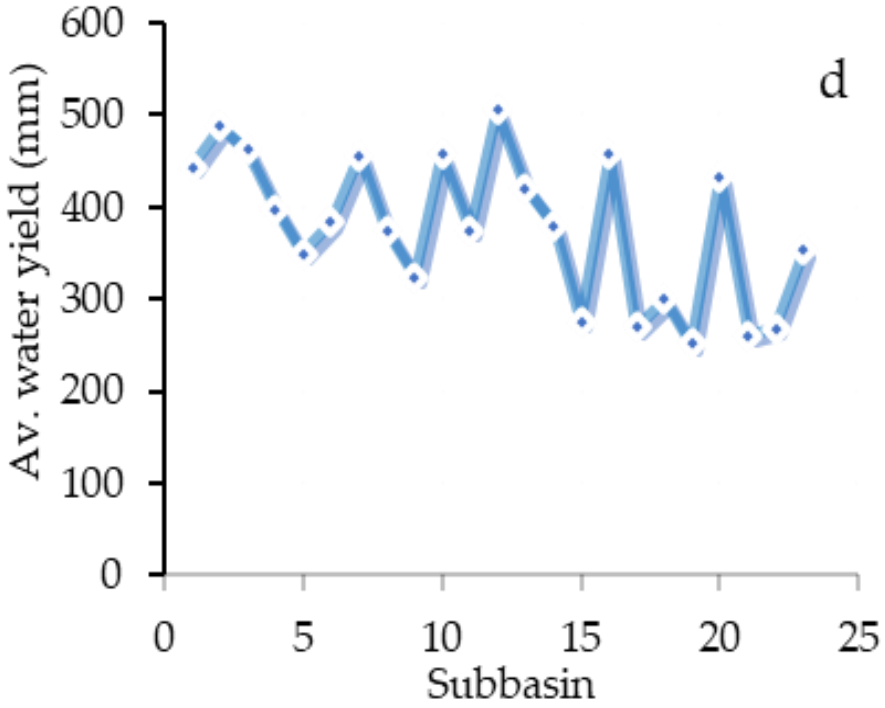

(d) Water yield in each sub-basin from 1998 to 2013 of catchment area

Figure 7 Hydrology and Water Yield of Catchment Area

From Figure 7b, it is evident that the catchment receives its highest rainfall between March and May and between August and November, with January being the driest month of the year. Therefore, the average water available in the catchment area is 29,900 M cm^3 which implies that there is sufficient water for irrigation in the catchment area. However, the problem is with the management strategies. Similarly, the annual average hydrological processes, including evaporation, infiltration, etc., are presented in the Table 3. Water yield accounts for the difference between the total rainfall and evapotranspiration in

the watershed. There was observed low water yields, rainfall, and varying crop water requirements in the catchment during the dry months of the year; June-July, and December-February (Figure 7c and Figure 7b) and following the subsequent reduction in rainfall and vice versa. Therefore, irrigation in the scheme is only needed during dry seasons and in months when rainfall is low.

Table 3 The water balance ratios

Processes	Average annual output (mm)
Precipitation	1087.8
Percolation to the shallow aquifer	2.32
Lateral flow	252.54
Surface Runoff	102.59
Return flow	26.91
Evaporation and transpiration	685.2
Potential evapotranspiration	2054.6
Evaporation from the shallow aquifer	12.86

Likewise, the curve number is a hydrological parameter broadly used and an effective method for determining the approximate amount of direct runoff from the rainfall event in the Scheme (Melesse and Graham, 2004). The scheme had a curve number of 75.35, indicating a high or increased runoff potential, an implication of high-water availability in the Doho rice scheme since, the higher the curve number, the less permeable the soil is (Figure 7a). Further, the percolation rate of the paddy fields of the study area seems to be relatively low due to location of the watershed in a downstream area and the soil in the paddy field is black clay with low infiltration rates. The percentage of the estimated flow rate to rainfall amount was 41%, and the percentage of the observed flow rate to the rainfall amount was 45% during calibration. Also, the stream recharge due to seepage was 12.86 mm. Percolation in paddy fields is affected by various factors including, soil type, regional drainage capacity (including groundwater level), water level of the drainage channel, the interaction of ponding depth in the paddy field with the depth of the surrounding paddy fields, and the condition of the hard pan and ridges (Sakaguchi et al., 2014). Additionally, average water yield and stream flow from 2000 to 2008 showed no flow reductions or declines in water yields (Figure 7c).

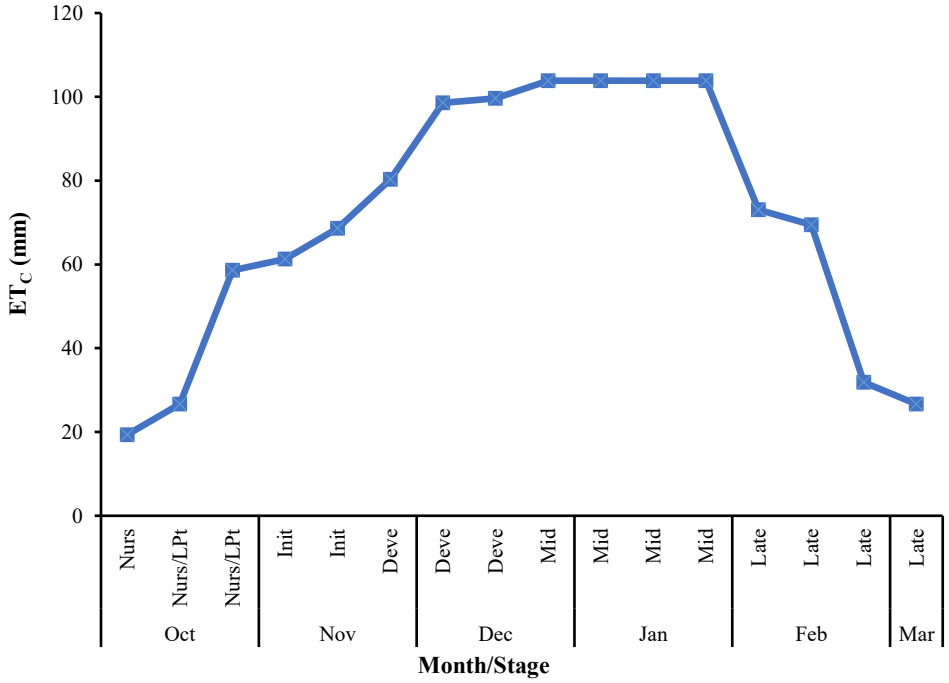

Figure 8 Paddy water requirement under each development stage

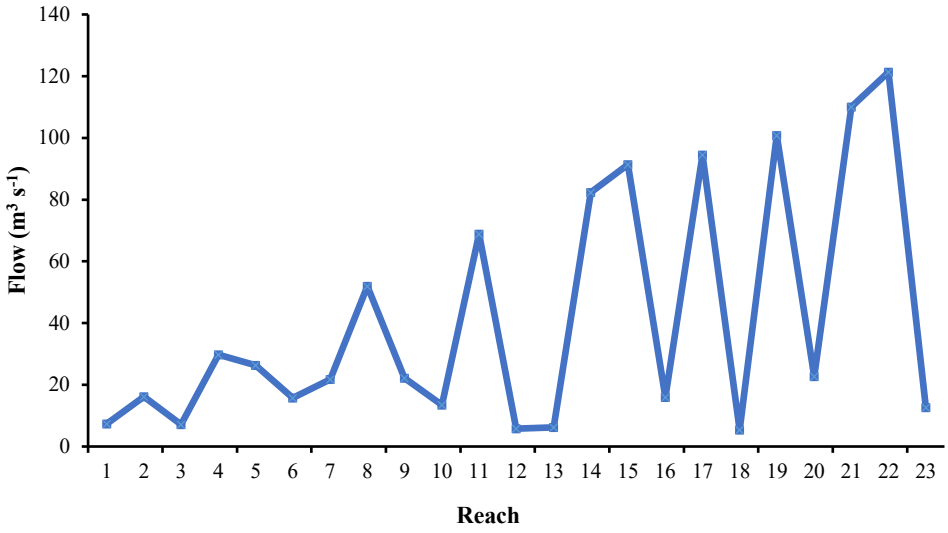

(a) Available water in each reach

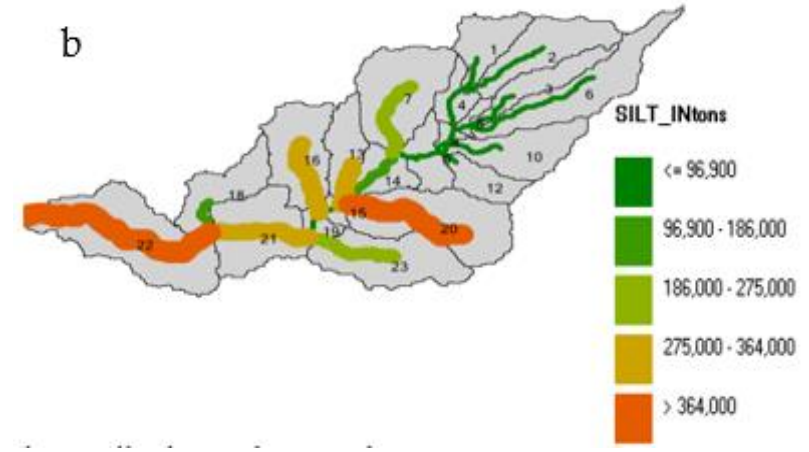

(b) Sediments in each reach before implementation of grassed waterways and desiltation

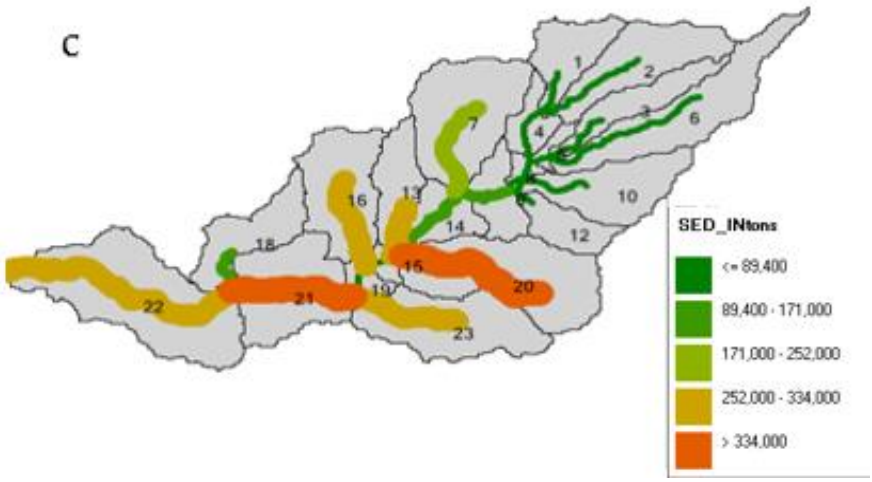

(c) Sediment reduction in reach 22 after implementation of grassed waterways and desiltation

Figure 9 Available Water and Sediment per Reach

3.3 The paddy water requirement

The average annual crop water needs for season one was 1129.6 mm (Figure 8), and the average rice water requirement in the Doho rice scheme for this season (Oct-Mar) annually was 11.053 Mm^3. The crop water requirement for season two (Oct-Mar) varied according to the rice growth stages (Figure 8). Based on the precipitation data (1st Jan 1999 to 31st Dec 2013), water evapotranspiration is high during crop development which ranges from 98.5 mm to

103.9 mm per decade. The seasonal average ET_c value for Oct-March was 57 mm per year. It can be noted that with the precipitation data in the model, the available water during the driest season cannot meet the crop water requirements.

3.4 Irrigation water management scenarios

The pothole impoundment module was implemented in the model. The results obtained in the hydrological cycle (Figure 7a) were used to estimate the water storage in the pothole. The implementation of the pothole module showed that the available water in the catchment was 126 m^3 s^{-1} compared to 945.5 m^3 s^{-1} (a) of the total available water from each basin in the catchment area. This is true and helps to improve the allocation of available irrigation water and use in Doho Rice Scheme by the farmers in the different blocks during the dry season. The size of the pothole was established to be of radius 8m and recommended for every block.

Additionally, desiltation and grassed waterways were implemented to reduce erosion (c). From the SWAT output viewer in the model, it was evident that the sediment reduced by a significant value of 36%, at sub-basin 22 (c), which is essential for improving water use and management in the scheme.

4 Conclusions

The current population growth in Uganda and the region pushes governments to increase rice production by rehabilitating large schemes (Bwire et al., 2022b). Water remains a key factor in contributing to food security and improved livelihoods. However, developing an integrated effective water use and management strategies at scheme levels to mitigate the intensifying climate change events including droughts are required (Bwire et al., 2025). In this study, the SWAT model simulated the hydrological processes and evaluated water availability and sustainable irrigation management practices in paddy HRUs of the catchment area. Calibrations and validation results improved the performance of desiltation-grass waterways in large paddy patches of the watershed.

Although the model required significant data and detailed analysis, the hydrological assessment at the catchment was performed. The model was helpful in the estimation of the available water, and the annual average volume of water recorded as 29900 M cm^3 at the Doho head works for the whole Manafwa catchment. The paddy crop water requirement was calculated, and the annual average crop requirement was 11.053 M m^3 for the whole catchment. Three water management scenarios were defined, including implementing the pothole impoundment module, desiltation and grassed waterways. Firstly, suggestion of placing of concrete pothole of 8m radius in all Doho rice scheme blocks, secondly implementing the grassed waterways and sediment removal in water for all irrigation canals within the scheme blocks. This reduced sedimentation and silt from 453191.7082 tons ha^{-1} to 292207.9526 tons ha^{-1} with a significant percentage reduction of 36%, which is vital in improving the water losses within the canals.

Such analyses are important and provide a sound scientific contribution in developing national irrigation and water management plans and policies to enhance rice production in the paddy ecosystem. Finally, integrating such measures in irrigation scheme designs and improving agricultural data availability can significantly boost research innovations in irrigation water-use, management and increase irrigation efficiency and crop productivity.

References

Abbaspour, K. C., E. Rouholahnejad, S. Vaghefi, R. Srinivasan, H. Yang, and B. Kløve. 2015. A continental-scale hydrology and water quality model for Europe: Calibration and uncertainty of a high-resolution large-scale SWAT model. *Journal of Hydrology*, 524: 733–752.

Akoko, G., T. H. Le, T. Gomi, and T. Kato. 2021. A review of SWAT model application in Africa. *Water*, 13(9): 1313.

Angella, N., S. Dick, and B. Fred. 2014. Willingness to pay for irrigation water and its determinants among rice farmers at Doho Rice Irrigation Scheme (DRIS) in Uganda. *Journal of Development and Agricultural Economics*, 6(8): 345–355.

Arnold, J. G., D. N. Moriasi, P. W. Gassman, K. C. Abbaspour, M. J. White, R. Srinivasan, C. Santhi, R. D. Harmel, A. van Griensven, M. W. Van Liew, N. Kannan, and M. K. Jha. 2012. SWAT: Model use, calibration, and validation. *Transactions of the ASABE*, 55(4): 1491–1508.

Bouslihim, Y., A. Rochdi, N. E. A. Paaza, and L. Liuzzo. 2019. Understanding the effects of soil data quality on SWAT model performance and hydrological processes in Tamedroust watershed (Morocco). *Journal of African Earth Sciences*, 160: 103616.

Bwambale, E., P. Gathogo Home, J. Messo Raude, and J. Wanyama. 2019. Development of a water allocation model for equitable water distribution at doho rice irrigation scheme, Uganda. *Hydrology*, 7(4): 62-69.

Bwire, D., H. Saito, R. C. Sidle, and M. Mugisha 2025. Water management for rice production: a key component of food security in East Africa. *Discover Water*, 5(1):7.

Bwire, D., H. Saito, M. Mugisha, and V. Nabunya. 2022a. Water productivity and harvest index response of paddy rice with alternate wetting and drying practice for adaptation to climate change. *Water*, 14(21): 3368.

Bwire, D., H. Saito, and E. Okiria. 2022b. Analysis of the impacts of irrigation practices and climate change on water availability for rice production: A case in Uganda. *Journal of Arid Land Studies*, 32(S): 123–127.

Bwire, D., F. Watanabe, and S. Suzuki. 2017. The Current Status and Issues of Irrigation Agriculture in Uganda. In *Proc. of Japanese Association of Arid Land Studies Symposium*, Pg 56. Tokyo, Japan, 27-28 May 2017.

CARD. 2019. SWAT Literature Database. Available at: https://www.card.iastate.edu/swat_articles/readme/. Accessed 25 March 2022.

Chen, S. K., C. S. Jang, S. M. Chen, and K. H. Chen. 2013. Effect of N-fertilizer application on return flow water quality from a terraced paddy field in Northern Taiwan. *Paddy and Water Environment*, 11: 123–133.

Dechmi, F., J. Burguete, and A. Skhiri. 2012. SWAT application in intensive irrigation systems: Model modification, calibration and validation. *Journal of Hydrology*, 470: 227–238.

Donmez, C., O. Sari, S. Berberoglu, A. Cilek, and O. Satir. 2020. Improving the applicability of the SWAT model to simulate flow and nitrate dynamics in a flat data-scarce agricultural region in the Mediterranean. *Water*, 12(12): 3479.

Erima, G., I. Kabenge, A. Gidudu, Y. Bamutaze, and A. Egeru. 2022. Differentiated spatial-temporal flood vulnerability and risk assessment in Lowland Plains in Eastern Uganda. *Hydrology*, 9(11): 201.

FAO. 1989. Irrigation Water Management: Irrigation Scheduling. Available at: http://www.fao.org/3/T7202E/t7202e00.htm#dataContent. Accessed 25 March 2022.

FAOSTAT. 2018. Food and agriculture data. Available at: https://www.fao.org/faostat/en. Accessed 27 May 2022.

Gassman, P. W., M. R. Reyes, C. H. Green, and J. G. Arnold. 2007. The soil and water assessment tool: historical development, applications, and future research directions. *Transactions of the ASABE*, 50(4): 1211–1250.

Gassman, P. W., A. M. Sadeghi, and R. Srinivasan. 2014. Applications of the SWAT model special section: overview and insights. *Journal of Environmental Quality*, 43(1): 1–8.

Geza, M., and J. E. McCray. 2008. Effects of soil data resolution on SWAT model stream flow and water quality predictions. *Journal of Environmental Management*, 88(3): 393–406.

Harmel, R. D., P. K. Smith, K. W. Migliaccio, I. Chaubey, K. R. Douglas-Mankin, B. Benham, S. Shukla, R. Muñoz-Carpena, and B. J. Robson. 2014. Evaluating, interpreting, and communicating performance of hydrologic/water quality models considering intended use: A review and recommendations. *Environmental Modelling & Software*, 57: 40–51.

Hoekstra, A. Y., M. M. Mekonnen, A. K. Chapagain, R. E. Mathews, and B. D. Richter. 2012. Global monthly water scarcity: blue water footprints versus blue water availability. *PloS One*, 7(2): e32688.

Hong, S., S. Hwang, J. Lamo, D. Nampamya, and T. S. Park. 2021. The current status of opportunities for rice cultivation in Uganda. *Journal of the Korean Society of International Agriculture*, 33(1): 67-74.

Kajonphol, T., N. Seetaput, M. Precharattana, and C. Sangsiri. 2018. Correlation and multiple regression model for economic traits of local rice (*Oryza sativa* L.) in upland rice system. *Applied Mechanics and Materials*, 879: 71–77.

Katic, P. G. 2014. Improving West African rice production with agricultural water management strategies. In *Global Water: Issues and Insights*, eds. R. Q. Grafton, P. Wyrwoll, C. J. White, and D. Allendes, ch. 6, 27–32. Canberra, Australia: ANU Press.

Kim, K., G. Whelan, S. T. Purucker, T. F. Bohrmann, M. J. Cyterski, M. Molina, Y. Gu, Y. Pachepsky, A. Guber, and D. H. Franklin. 2014. Rainfall–runoff model parameter estimation and uncertainty evaluation on small plots. *Hydrological Processes*, 28(20): 5220–5235.

Liyantono, T. Kato, H. Kuroda, and K. Yoshida. 2013. GIS

analysis of conjunctive water resource use in Nganjuk district, east Java, Indonesia. *Paddy and Water Environment*, 11: 193–205.

Materu, S. T., S. Shukla, R. P. Sishodia, A. Tarimo, and S. D. Tumbo. 2018. Water use and rice productivity for irrigation management alternatives in Tanzania. *Water*, 10(8): 1018.

McCuen, R. H., Z. Knight, and A. G. Cutter. 2006. Evaluation of the Nash–Sutcliffe efficiency index. *Journal of Hydrologic Engineering*, 11(6): 597–602.

Melesse, A. M., and W. D. Graham. 2004. Storm runoff prediction based on a spatially distributed travel time method utilizing remote sensing and GIS. *JAWRA Journal of the American Water Resources Association*, 40(4): 863–879.

Moriasi, D. N., J. G. Arnold, M. W. Van Liew, R. L. Bingner, R. D. Harmel, and T. L. Veith. 2007. Model evaluation guidelines for systematic quantification of accuracy in watershed simulations. *Transactions of the ASABE*, 50(3): 885–900.

Mwaura, F. M., and F. R. Muwanika. 2018. Providing irrigation water as a public utility to enhance agricultural productivity in Uganda. *Utilities Policy*, 55: 99–109.

MWE. 2012. Proposed institutional arrangements and regulatory framework for sustainable management of irrigation schemes implemented under FIEFOC project. Kampala, Uganda: Ministry of Water and Environment.

Nagelkerke, N. J. D. 1991. A note on a general definition of the coefficient of determination. *Biometrika*, 78(3): 691–692.

Namyenya, A., D. Serunkuuma, and F. Bagamba. 2014. Willingness to pay for irrigation water and its determinants among rice farmers at Doho Rice Irrigation Scheme (DRIS) in Uganda. *Journal of Development and Agricultural Economics,* 6(8): 345-355.

Nash, J. E., and J. V. Sutcliffe. 1970. River flow forecasting through conceptual models part I—A discussion of principles. *Journal of Hydrology*, 10(3): 282–290.

Neitsch, S. L. 2005. SWAT2005 theoritical documantation. https://swat.tamu.edu/media/1292/SWAT2005theory.pdf. Accessed 15 February 2022.

OECD & FAO. 2022. OECD-FAO agricultural outlook 2022-2031. OECD Publishing, Paris, France.

Onen, P., E. Opolot, G. Aguttu, and G. Olupot. 2022. Optimizing water use efficiency in flood irrigation systems in uganda: a case of doho rice irrigation scheme (dris). In *2nd African Conference on Precision Agriculture (AfCPA)*, 168-172. Benguérir, Morocco, 7-9 December 2022.

Otim, D., J. Smithers, A. Senzanje, and R. van Antwerpen. 2020. Verification of runoff volume, peak discharge and sediment yield simulated using the ACRU model for bare fallow and sugarcane fields. *Water SA*, 46(2): 182–196.

Ouyang, W., P. Wei, X. Gao, R. Srinivasan, H. Yen, X. Xie, L. Liu, and H. Liu. 2020. Optimization of SWAT-Paddy for modeling hydrology and diffuse pollution of large rice paddy fields. *Environmental Modelling and Software*, 130: 104736.

Prodhan, Z. H., and Q. Shu. 2020. Rice aroma: A natural gift comes with price and the way forward. *Rice Science*, 27(2): 86–100.

Sakaguchi, A., S. Eguchi, T. Kato, M. Kasuya, K. Ono, A. Miyata, and N. Tase. 2014. Development and evaluation of a paddy module for improving hydrological simulation in SWAT. *Agricultural Water Management*, 137: 116–122.

Santhi, M. H., G. M. S. Knight, and K. Muthumani. 2005. Evaluation of seismic response of soft-storey infilled frames. *Computers and Concrete*, 2(6): 423–437.

Schulze, R. E. 2011. A 2011 perspective on climate change and the South African water sector. WRC Project No. K5/1843. Gezina, South Africa: Water Research Comission.

Song, X., J. Zhang, C. Zhan, Y. Xuan, M. Ye, and C. Xu. 2015. Global sensitivity analysis in hydrological modeling: Review of concepts, methods, theoretical framework, and applications. *Journal of Hydrology*, 523: 739–757.

Supakosol, J., and K. Boonrawd. 2020. Hydrologic evaluation and effects of climate change on the Nong Han Lake Basin, northeastern Thailand. *Journal of Water and Climate Change*, 11(4): 992–1000.

Tang, X., J. Zhang, G. Wang, J. Jin, C. Liu, Y. Liu, R. He, and Z. Bao. 2021. Uncertainty analysis of SWAT modeling in the lancang river basin using four different algorithms. *Water*, 13(3): 341.

The Nature Conservancy. 2023. *Hydrologic Response Units*. Available at: https://www.stormwaterheatmap.org/docs/Data Layers/hydrologic_response_units. Accessed 25 March 2022.

Tsuchiya, R., T. Kato, J. Jeong, and J. G. Arnold. 2018. Development of SWAT-paddy for simulating lowland paddy fields. *Sustainability*, 10(9): 3246.

Tuppad, P., N. Kannan, R. Srinivasan, C. G. Rossi, and J. G. Arnold. 2010. Simulation of Agricultural Management Alternatives for Watershed Protection. *Water Resources Management*, 24: 3115-3144.

USDA. 2023. Economic Research Service, Situation and Outlook. Available at: http://www.worldagriculturalproduction.com/crops/rice.aspx. Accessed 25 September 2023.

Van Griensven, A., P. Ndomba, S. Yalew, and F. Kilonzo. 2012. Critical review of SWAT applications in the upper Nile basin countries. *Hydrology and Earth System Sciences*, 16(9): 3371–3381.

Wei, R., and W. Zimmermann. 2017. Biocatalysis as a green route for recycling the recalcitrant plastic polyethylene terephthalate. *Microbial Biotechnology*, 10(6): 1302–1307.

Xie, X., and Y. Cui. 2011. Development and test of SWAT for modeling hydrological processes in irrigation districts with paddy rice. *Journal of Hydrology*, 396(1–2): 61–71.